Formation of calcite in the presence of dissolved organic matter: partitioning, fabrics and fluorescence

Andrew R. Pearson[1*], Adam Hartland[1], Silvia Frisia[2], Bethany R.S. Fox[3,1].

[1] Environmental Research Institute, School of Science, Faculty of Science and Engineering, University of Waikato, Hamilton, 3216, New Zealand.

[2] School of Environmental and Life Sciences, The University of Newcastle, Callaghan, New South Wales, 2308, Australia.

[3] Department of Biological and Geographical Sciences, University of Huddersfield, Huddersfield, HD1 3DH, United Kingdom.

*Corresponding author: apearson181@gmail.com

Declarations of interest: none.

Key words: dissolved organic matter (DOM); calcite; calcite fabric; carbonate; flowstone; 3D EEM (excitation emission matrix) fluorescence.

Abstract

Dissolved organic matter (DOM) is omnipresent in natural waters and is commonly incorporated into carbonates. Records of DOM from speleothems (secondary carbonates found in caves) have often been interpreted to reflect groundwater DOM concentrations. However, the fidelity of these records is largely untested. An understanding of the relationship between dripwater and speleothem DOM is thus required to allow speleothems to be reliably used as archives of DOM concentration.

We precipitated calcite ($CaCO_3$) crystals from weak solutions of $(NH_4)_2CO_3$, $CaCl_2$ and NH_4Cl. These solutions also contained peat DOM (from 0 to 15 mgC/L~~ppm~~). Fluorescence 3D excitation-emission matrix (3D EEM) analysis showed a strong, positive correlation between [DOM] in the parent-solution~~aq~~, and [DOM]~~calcite~~ in the calcite. Calcite precipitation was reduced at high DOM concentrations, potentially indicating inhibition of crystallisation. Partition coefficient values showed that DOM_{aq} was subtly preferentially incorporated into calcite.

Scanning electron microscope images indicated that the crystal structures were heavily influenced by DOM adsorption with finer, smooth-faced, rhombohedral crystals forming in growth solutions with low aqueous [DOM]~~aq~~ (0-5 mgC/L~~ppm~~), and prismatic, 'impure' crystals produced at high aqueous [DOM]~~aq~~ (10 and 15 mgC/L~~ppm~~).

Overall, our results indicate that authigenic carbonates are likely to faithfully record variations in aqueous [DOM]~~aq~~ within the natural range of DOM concentrations in representative freshwater systems (caves, soil water), and that crystal habits are altered by aqueous [DOM]~~aq~~ within their growth solutions.

We also applied our findings to three flowstones collected from three New Zealand caves which vary in climatic, vegetation and hydrological regimes. We conclude that differences in

initial aqueous [DOM]$_{aq}$ do indeed control incorporation of DOM into calcite, and thus 3D EEM fluorescence can be used to reconstruct original aqueous [DOM]$_{aq}$ from authigenic carbonates.

1. Introduction

The organic matter (OM) components in soil contain more than three times as much carbon as either the Earth's atmosphere or terrestrial vegetation and are sensitive to climatic and environmental changes (Schmidt et al., 2011). Soil organic matter (SOM) is a heterogenous assortment of organic compounds ranging from intact plant materials to highly oxidised carbon in carboxylic acids at different degradation stages (Lehmann and Kleber, 2015), and also includes microbial biomass. Soil organic matter can adhere to and be strongly mixed with soil minerals, and therefore the number of compounds that may constitute soil organic matter is effectively limitless, and no single chemical description can be given (Evans et al., 2005). A fraction of soil organic matter is soluble and can be transported in dissolved or colloidal form into groundwater (Hartland et al., 2012). Dissolved organic matter is ubiquitous in natural environments and is arbitrarily defined as organic matter with particle sizes below 0.45 µm. "Dissolved" organic matter is therefore a misnomer, as colloidal particles can exist down to 1 nm (Lead and Wilkinson, 2006). However, since it is the conventional term for this class of organic matter, we will be using it throughout this paper.

DOM is highly complex and includes a diverse range of aromatic and aliphatic hydrocarbon structures that may have attached functional groups (Leenheer and Croué, 2003). In terrestrial waterbodies, DOM can affect biodiversity and ecological processes (Rae et al., 2001), contribute to global climate change via degassing as CO_2 and CH_4 (following degradation reactions (Cole et al., 1994; Cole et al., 2007; Mayorga et al., 2005)), and act as a vector for trace metal transport (Hartland et al., 2012; Sauve et al., 2000). DOM can precipitate out of

waterbodies in mineral phases (e.g. in biogenic or abiogenic carbonate precipitates) or be deposited in sediments. Herein, $[DOM]_{aq}$ and $[DOM]_s$ refer to the aqueous (i.e. in solution) and solid phase (i.e. incorporated in calcite, the rhombohedral phase of $CaCO_3$) dissolved organic matter concentration, respectively. ~~Routine monitoring of DOM in terrestrial waterbodies (as dissolved organic carbon (DOC)), began in the mid-late 20th century (e.g. the Acid Monitoring Network, UK (Monteith et al., 2014)).~~ Little is known about DOM trends prior to the onset of widespread dissolved organic carbon (DOC) monitoring, which became routine in several countries the mid-late 20th century (e.g. the Acid Monitoring Network, UK (Monteith et al., 2014)). ~~Yet, An~~an ongoing debate surrounds the causes of recent (late 20th century to present) DOM increases in terrestrial waterbodies in mid/high-latitudes of the Northern Hemisphere (Evans et al., 2006; Monteith et al., 2007) (the Southern Hemisphere is comparatively understudied). Proposed contributing factors include ~~climate change~~increasing temperatures (Freeman et al., 2001), changes in soil water acidity due to declining atmospheric sulphur deposition (Evans et al., 2006; Monteith et al., 2007) elevated atmospheric CO_2 concentrations (causing stimulation of primary productivity) (Freeman et al., 2004), and changes in land-use (Stanley et al., 2012). This debate may be resolved using long-term (centennial to millennial-scale) records of DOM variability encoded in natural sedimentary or mineralogical archives, which may allow the isolation and assessment of individual potential contributing factors.

One of the most promising environmental archives is that of speleothems, secondary calcium carbonate deposits typically found in caves (e.g. flowstones and stalagmites) (Hill et al., 1997). Inorganic geochemical properties (isotopic and trace element data) (Affolter et al., 2019; Nagra et al., 2017; Scroxton et al., 2018; Williams et al., 1999) and physical properties (e.g. nano-crystal aggregation, open vs. compact columnar fabrics, defect-ridden fabrics) of natural calcium carbonate minerals have been routinely used to determine environmental

parameters at~~of~~ their time of formation (Frisia et al., 2000; Nielsen et al., 2014). Speleothems can preserve organic molecules from overlying allochtonous vegetation, soil and microbial communities within the cave (Blyth et al., 2016). ~~Speleothems record multi-proxy information about climatic and environmental changes in their physical and chemical properties and in many cases~~ The precision and reliability of speleothem dating means that~~an be precisely dated to~~ palaeo-environmental records containing seasonal/monthly resolutions can be produced, extending to hundreds of thousands of years (Borsato et al., 2007). Speleothems thus have the potential to record DOM trends prior to anthropogenic land-use impacts and anthropogenically induced fluctuations in atmospheric S deposition, two factors that have been proposed as contributing drivers of recent increases in DOM export from soil.

~~Soil organic matter is a heterogenous assortment of organic compounds ranging from intact plant materials to highly oxidised carbon in carboxylic acids at different degradation stages (Lehmann and Kleber, 2015), and also including microbial biomass. Soil organic matter can adhere to and be strongly mixed with soil minerals, and therefore the number of compounds that may constitute soil organic matter is effectively limitless, and no single chemical description can be given (Evans et al., 2005). A fraction of soil organic matter is soluble and can be transported in dissolved or colloidal form into groundwater (Hartland et al., 2012).~~ Slightly acidic groundwater ~~may~~ dissolves limestone bedrock and thus transport both soil organic matter and calcium (Ca^{2+}) and carbonate (CO_3^{2-}) ions into cave systems. There, ions are reprecipitated as solid calcium carbonate, forming speleothems. During this process, soil-derived organic matter (including DOM) may be incorporated into the speleothem $CaCO_3$ (Baker et al., 1999; Genty et al., 2001). Organic matter has long been known to alter speleothem colour (Caldwell et al., 1982): dark coloured speleothems are known to contain greater amounts of particulate organic matter (POM), fulvic acid (FA) and humic acid (HA) compared to light-coloured speleothems (Van Beynen et al., 2001). Several studies (Chalmin

et al., 2012; Quiers et al., 2015) have observed that humic acid fluoresces more strongly after incorporation into calcite, which suggests an interaction between humic acid molecules and the crystal lattice (fluorescence yields increase when molecules adopt more rigid conformations) (Sulatskaya et al., 2010), such as surface adsorption of organic molecules, and bonding between organic functional groups (e.g. carboxyl (COO^-) and cations (Ca^{2+}) (Fairchild and Baker, 2012; Hartland et al., 2014). It has also been suggested that organic matter may be incorporated into speleothems as fluid inclusions (Ramseyer et al., 1997). Blyth et al. (2016) reviewed the origin, transport and transformation of OM in speleothems and suggested that speleothem OM is primarily derived from vegetation or soil overlying the cave. An important consideration is that dripwater OM can be altered during transport, prior to being preserved in a speleothem. For example, speleothems fed by water with a long-residence time are likely to contain OM that has been heavily altered (e.g. by microbial activity) along the flow-path.

A small fraction of DOM is fluorescent and is typically described as fluorescent dissolved organic matter (FDOM). Three-dimensional excitation emission matrix (3D EEM) fluorescence can be used to quantify and characterise FDOM properties (Coble, 1996; Stedmon and Bro, 2008). When fluorescence conforms to the Beer–Lambert ~~Beer-Lambert~~ law (i.e. the amount of light absorbed by a solution is proportional to the solution's molar absorptivity and the concentration of solute), mathematical identification (i.e. PARAFAC-parallel factor analysis of components) can be used to quantify and characterise analytes (Murphy et al., 2013), including DOM concentration and constituent molecules, by assessing fluorophore intensity and the wavelengths at which excitation and emission occur. Fluorescence methods (but not necessarily 3D EEMs) have been applied to assess DOM quantity and quality in speleothems and cave drip-waters in a diverse range of environmental and palaeo-environmental studies. Examples include studies of DOM loss and processes in

the overlying soil (Genty et al., 2001; Perrette et al., 2015), land-use change (Blyth et al., 2007) and vegetation change (Baker et al., 1996). Several studies have also focused on the relationship between trace-metal-DOM complexation in cave dripwaters and speleothems (Hartland et al., 2012; Rutlidge et al., 2014).

Here, we aim to test (a) whether secondary calcium carbonate is a faithful recorder of $[DOM]_{aq}$ and (b) the effect of $[DOM]_{aq}$ on calcium carbonate crystal morphology and lattice defects. We test this by precipitating calcium carbonate in solutions containing varying concentrations of DOM (approximately 0, 5, 10, 15 mgC/L~~ppm~~). Our calcite crystals were synthesised using an adapted Gruzensky protocol (Gruzensky, 1967), in which NH_3 and CO_2 gases are sublimed from ammonium carbonate and diffuse into an aqueous solution of calcium and ammonium chloride, causing supersaturation and precipitation of $CaCO_3$. Laboratory experiments exclude the complexities of changes in water chemistry, DOM characteristics, interactions with trace elements and potential microbial activity that may influence crystallisation pathways in the cave environment, therefore enabling us to simply test the effects of natural [DOM] on crystallisation processes and the relationship between $[DOM]_{aq}$ and $[DOM]_s$.

Most laboratory studies that focus on incorporation of organic impurities in calcite have relied on laboratory grade humic acids (Chalmin et al., 2012; Falini et al., 2009) or isolation of individual organic ligands (Mavromatis et al., 2017). However, carbonate precipitation in natural environments occurs with a range of organic molecules that may be altered by natural processes (e.g. microbial degradation, decomposition). In this study, we aimed to address this issue by using natural DOM sourced from Kopuatai peat dome, a raised bog in central North Island, New Zealand. We also used the same fluorescence methods to test the reliability of three flowstones to record DOM concentrations from their parent dripwaters at three different cave sites in New Zealand.

2. Materials and Methods

2.1. Experimental design

The carbonate precipitation experiment applied a range of methods to analyse the growth-solutions and the carbonate produced under the different experimental conditions (Fig. 1a).

Flame atomic absorption spectroscopy (FAAS) was used to determine the loss of calcium ions from the growth solution through time, whilst 3D EEM spectroscopy was used to measure removal of DOM through time. Post-experiment, 3D EEM spectroscopy was used to quantify [DOM] from the dissolved crystals, the morphology of the crystal habits was assessed using scanning electron microscopy (SEM), whilst the polymorph of the crystals was determined using Fourier transform infrared spectroscopy (FTIRS) and X-ray diffraction (XRD) (Fig. 1a). To assess the relevance of the experimental findings in a natural environment, [DOM] in dripwaters and flowstones from three caves were measured and compared using 3D EEM spectroscopy (Fig. 1b).

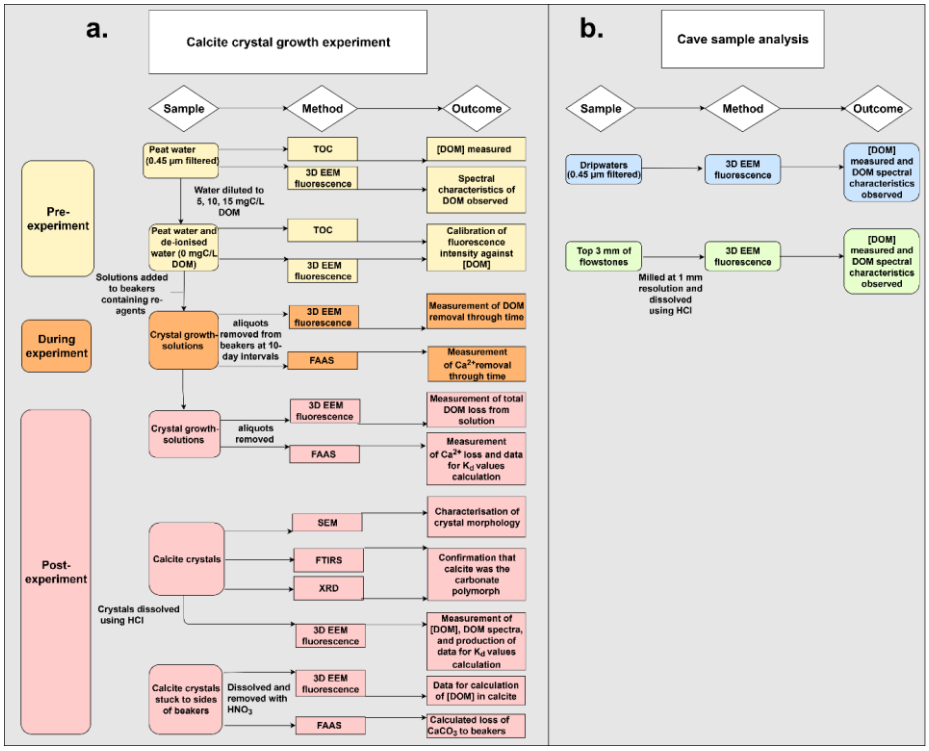

Fig. 1. (a.) Flowchart showing the experimental plan for the calcite crystal growth experiment. **(b.)** Flowchart showing the experimental plan for analysis of the dripwaters and flowstones from the cave. sites.

Peat water was chosen as the growth solution for our experiment because it contains high concentrations of DOM (enabling dilution to the concentrations required in our experiment). Peat-derived DOM is also relevant to cave research: several studies have analysed the fluorescence of dripwaters and speleothems in caves located beneath peat bogs (Baker et al., 1999; Charman et al., 2001). Water was pumped from a depth of approximately 20 m from Kopuatai, a raised bog (10,000 ha.) located in the Hauraki Plains, a lowland, temperate zone in the Waikato region, central North Island, New Zealand (Ratcliffe et al., 2019). After collection, the water was stored in the dark at 4 °C. ~~Peat water was chosen as the growth solution for our experiment because it contains high concentrations of DOM (enabling~~

Field Code Changed

[illegible]

The Kopuatai water was filtered through 0.45 µm cellulose-acetate syringe filters (Microanalytix Pty Ltd, Australia), and analysed for total organic carbon (TOC). Prior to the experiment, the dissolved organic carbon (DOC) concentration of the filtered peat-solution was analysed using an O-I Analytical Aurora 1030W TOC analyser, using the standard heated persulfate wet-oxidation method, whereby organic compounds are oxidised by high-temperature $Na_2S_2O_8$ to measure non-purgable organic carbon (NPOC) as TOC. Sample measurements were calibrated against standards of dilute potassium hydrogen phthalate (KHP) prepared using 18.2 MΩ water. Because the solution was filtered at 0.45 µm (and therefore classified as "dissolved"), TOC values will henceforth be referred to as DOM values. The peat-water was found to have a DOM concentration of 30 mgC/L, which is higher by a factor of ~2 than typically found in cave dripwaters. The peat water was diluted with deionised water to produce solutions containing ~5 mgC/L, ~10 mgC/L, and ~15 mgC/L DOM (Table 1; henceforth referred to as low, medium and high [DOM] treatments respectively). Two experimental blanks (~ 0 mgC/L DOM) were prepared from 18.2 MΩ water.

$CaCl_2$ (284.44 g/L) and NH_4Cl (2.66 g/L) were added to the growth solutions. 100 mg of reagent grade calcite (BDH laboratories Ltd.) was added to each solution to act as seed crystals. Each 450 mL growth solution ~~had a final volume of 450 mL and were~~ was sealed in a 1000 mL acid-washed Pyrex beaker. Acid-washing involved soaking in ~~(~~ 10% HCl for 24 hours, followed by 24 hours in de-ionised water~~)~~. Solid ammonium carbonate~~s~~ $(NH_4)_2CO_3$ was added to glass vials, which were attached and sealed to the side of each Pyrex beaker (thus keeping the ammonium carbonate in contact with the headspace). The top of the beaker was ~~also~~ sealed gas-tight with lubricating grease (Glisseal), a glass plate, and rubber bungs

(Fig. 2~~1~~). Calcium carbonate crystals were precipitated via sublimation of CO_2 and NH_3 from $(NH_4)_2CO_3$ (55.5 g/L).

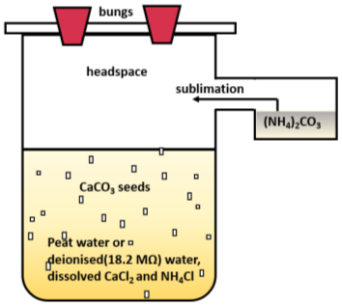

Fig. 2~~1~~. Experimental design for the carbonate precipitation experiment.

The presence of a headspace enabled supersaturation with respect to $CaCO_3$. The experiment was undertaken at a constant temperature of 21 °C in darkness. Upon completion of the experiment, suspended crystals were removed, rinsed with 18.2 M Ω water, oven dried at 40 °C overnight, and weighed. Crystals that were adsorbed to the beaker were removed via dissolution using known volumes of 5% HNO_3.

2.2 FAAS (flame atomic absorption spectroscopy) of growth solutions

Every 10 days throughout the experiment, 1 mL of solution was removed, diluted 100 times with 18.2 M Ω water and acidified to 2% HNO_3 prior to measurement of Ca^{2+} concentration by flame atomic absorption spectroscopy (FAAS) using a GBC Avanta flame atomic absorption spectrometer. These measurements were used to determine the loss of calcium ions from the solution over time and thus precipitation rates of $CaCO_3$. FAAS was also used to determine the loss of $CaCO_3$ by adsorption to beaker walls (via analysis of HNO_3 rinse solutions).

~~2.3 New Zealand flowstones~~

Crystals from each experimental treatment were ground into a fine powder and homogenised using a pestle and mortar. Aliquots of 2 mg (+/-2.5%) of each sub-sample were extracted, mixed and homogenised with 400 mg of oven-dried (100°C) KBr, before being compressed under 10,000 kg of pressure, forming translucent discs. Following the method of Ni and Ratner (2008), FTIR spectra were collected at a resolution of 1 cm^{-1} with eight scans ranging between 600–1200 wavenumbers (cm^{-1}) using a Perkin-Elmer Spectrum 100 spectrometer. Background measurements of a blank KBr disc were taken.

2.45. X-ray diffraction (XRD) of crystals

Following the method of Ni and Ratner (2008), aliquots of crystals from each treatment were ground into a fine powder prior to analysis on a Panalytical Empyrean XRD. Cu Kα radiation energy at 40 kV and 20 mA was used and the XRD patterns were collected at a scanning rate of 0.02 ◦/s in 2θ with diffraction angles ranging from 20 θ to 60 θ.

2.56. Scanning electron microscopy (SEM) of crystals

Aliquots of crystals collected from each beaker and a sample of the seed crystals (reagent grade calcium carbonate, 98%, Sigma Aldrich) were sputter coated in an ultra-thin layer of platinum and palladium to ensure sample conductivity. The coated crystals were attached to aluminium stubs using double-sided adhesive tape. Observations were carried out in scanning mode using a voltage of 5 kV on a Hitachi S-4700 cold field emission microscope, with the aim of analysing and describing any potential effects of [DOM] on calcite crystal structure. Working at low voltage (5 Kv) minimises sample damage by the beam and allows production of detailed surface images.

2.67. Fluorescence analysis of experimental growth solutions and calcite samples~~, crystals, and flowstone samples~~

Prior to the experiment, DOM solutions were measured for 3D excitation emission matrix fluorescence (3D EEM) using a Horiba Jobin Yvon Aqualog spectrometer with a 0.5 sec integration time, step-size of 3 nm, a measurement range of 240-600 nm excitation and 245-800 nm emission, and a CCD (charge-coupled device) detector. To correct for instrument specific biases (Stedmon and Bro, 2008), each matrix was corrected for inner-filter effects, scatter lines were Rayleigh masked, and spectra were then normalised to the mean Raman intensity of distilled deionised water (using the Aqualog's in-situ data processing software and protocols (Gilmore and Cohen, 2013)). EEM data were processed with MATLAB using parallel factor analysis (PARAFAC) as implemented in the N-way toolbox (Andersson and Bro, 2000), and the drEEM toolbox(Murphy et al., 2013). PARAFAC provides multi-way data analysis in which the underlying phenomena of fluorescence can be distinguished and separated into statistically valid components (Fellman et al., 2010; Ishii and Boyer, 2012).

During the experiment, 3D EEM analysis was used to measure quantitative DOM loss from solution at 10-day intervals, from day 10 onwards. 1 mL samples were removed from the growth solution and diluted by a factor of ten prior to analysis (approximately four mL of solution is required for 3D EEM analysis). At the end of the experiment, three 2 mg aliquots of the calcite crystals (from each beaker) were dissolved in 4.5 mL of 0.025 M HCl and analysed via the same 3D EEM fluorescence method as the solutions. This resulted in calcite digests with a final pH of ~5.6. The concentration of HCl used was selected to provide sufficient H^+ ions to dissolve the calcite whilst minimising the acidity of the final solutions for fluorescence analysis.

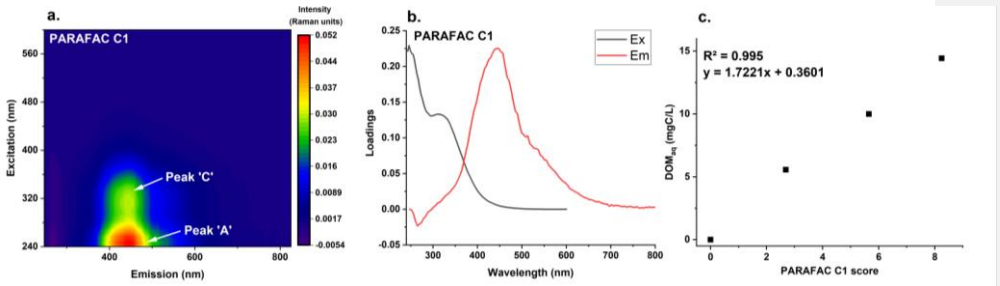

281

282 **Fig. ~~2~~3. (a.)** 3D excitation-emission matrix of PARAFAC component 1 (C1) **(b.)** Excitation and emission
283 loadings of PARAFAC component 1. **(c.)** Correlation between PARAFAC C1 score and DOM (mgC/L). The
284 equation was applied to C1 scores to calculate [DOM] throughout this experiment.

285 ~~The upper 3 mm of each natural cave flowstone was sampled at 1 mm resolution (Table A1),~~
286 ~~and each sample (5 mg calcite to 4 mL solution) was dissolved using the same method as the~~
287 ~~experimentally produced calcite.~~ The experimental samples (i.e. growth solutions and calcite)
288 and the cave samples (i.e. dripwaters and flowstones) were measured using the same
289 fluorescence method and data processing techniques. A one component PARAFAC model
290 was found to be most suitable for the peat-solutions and the dissolved experimental crystal
291 solutions, because only one meaningful fluorescence component (humic-like) was produced.
292 The fluorescence signal of the growth solution was dominated by humic-like fluorescence
293 peaks 'A' (ex 250-260; em 380-480) and 'C' (ex 330-350 nm; em 420-480) (Coble, 1996)
294 (Fig. 3~~2~~a, b). This two peak pattern is common in humic material from terrestrial
295 environments (Coble et al., 1998) including cave dripwaters (Hartland et al., 2010; Rutlidge
296 et al., 2014). The humic-like fluorescence intensity (PARAFAC Component 1 score)
297 measurements were regressed against DOM measurements, producing a strong, positive
298 correlation (R^2=0.99) (Fig. 3~~2~~c).

299

300 **2.7 New Zealand flowstones**

To assess how reliably cave calcite incorporates representative concentrations of DOM from their parent waters, three flowstones and their associated drip-waters obtained at three New Zealand cave sites were analysed using 3D EEM fluorescence. Flowstones are deposited from flowing films of water, and such films generally have a larger catchment area of contributing drips than is typical of stalagmites (Fairchild and Baker, 2012). Thus, flowstones are likely to provide a more representative archive of soil carbon leaching from above the cave than other types of cave deposit (Lechleitner et al., 2017). Further, Blyth et al. (2016) claimed that speleothems with a rapid-flow component (e.g. flowstones) are expected to have higher amounts of allochtonous OM than other speleothem types. The three studies sites (Fig. A4) span approximately seven degrees of latitude with accompanying changes in surface vegetative cover and surface temperature. From north to south: 38 °S sub-tropical podocarp forests (Waipuna Cave, Waitomo, N. Island); 40 °S temperate beech forest (Hodges Creek, Mt. Arthur Tablelands, Kahurangi National Park, S. Island) and 45 °S alpine tussock grassland (Dave's Cave, Mt. Luxmore, Fiordland, Southland, S. Island).

2.8. Determination of the partition coefficient of $[DOM]_{aq}$ to $[DOM]_s$

We used the fluorescence measurements from the growth solutions ($[DOM]_{aq}$) and corresponding dissolved calcite ($[DOM]_s$) to calculate the partition coefficient (i.e. efficiency of incorporation) of DOM from solution into calcite in each experimental treatment and from dripwaters to speleothem. We used the following formula:

$$K_d = (DOM_s/Ca_s) / (DOM_{aq}/Ca_{aq}) \quad (1.)$$

where K_d = partition coefficient, $_s$ = within calcite, and $_{aq}$ = within solution. All units are molar.

3. Results

3.1. Determining the calcium carbonate polymorph

FTIRS (Fig. 4~~3~~a) of the precipitated carbonate crystals displayed the characteristic $_{v2}$ band of calcite at 874cm^{-1} and the characteristic $_{v4}$ band of calcite at 713 cm^{-1}. These observations were in agreement with spectra obtained from pure calcite crystals (Ni and Ratner, 2008). XRD (Fig. 4~~3~~b) analysis displayed diffraction patterns that are consistent with calcite x-ray diffraction standards (Ni and Ratner, 2008).

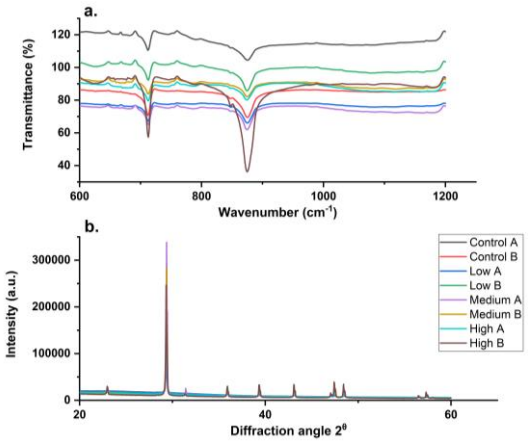

Fig. 4~~3~~. (a) FTIRS spectra of the carbonate crystals (KBr pellets) and **(b)** XRD analysis of crystal aliquots from each [DOM] treatment.

3.2. DOM incorporation into calcite crystals

Table 1 gives the fluorescence-inferred DOM and FAAS-inferred Ca^{2+} concentrations measured from growth solutions at day 10 and day 40 of the experiments, as well as the total mass of DOM incorporated into the calcite. PARAFAC component scores at day 10 were higher than those at day 0 for a number of the solutions, which at first glance suggests an increase in the organic carbon concentration. This was likely due to the addition of reagents as part of the experiment, resulting in an inner-filtering effect in the fluorescence measurements (thereby increasing fluorescence intensity values). To avoid confusion, initial

fluorescence intensities presented correspond to experimental solutions at day 10 rather than day 0.

DOM Treatment (A and B are replicates)	DOM_{aq} (mgC/L) (day 10)	DOM_{aq} (mgC/L) (day 40)	DOM_{aq} loss (mg) (day 10-40)	[1]PC1 (day 10)	[1]PC1 (day 40)	Ca^{2+} (mg/L) (day 0)	Ca^{2+} (mg/L) (day 40)	DOM_s (in $CaCO_3$) (mgC/L) (day 40)	Total $CaCO_3$ yield (mg) (day 40)	DOM_s (in $CaCO_3$) (mg) (day 40)	Log K_d values (day 40)	[2]Fractional difference	pH (day 40)
Control A	0.29	0.07	0.10	0.16	0.04	962.3	9	319	537	0.17	-0.43	1.74	8.45
Control B	0.17	0	0.10	0.09	-0.04	962.3	53.0	89	627	0.06	-0.11	0.55	8.17
Low A	5.46	4.79	0.30	3.07	2.7	962.3	264	529	493	0.26	0.63	0.87	7.27
Low B	4.93	4.70	0.20	2.77	2.64	962.3	68.1	543	824	0.45	0.58	2.22	7.96
Med A	9.28	7.52	0.79	5.22	4.23	962.3	37.2	1415	805	1.14	0.44	1.44	8.29
Med B	9.37	8.06	0.69	5.27	4.53	962.3	21	1429	916	1.31	0.44	1.90	8.35
High A	15.70	13.26	1.10	8.83	7.46	962.3	102	1849	464	0.86	0.55	0.78	7.70
High B	15.53	12.85	1.21	8.73	7.22	962.3	48.2	1737	396	0.69	0.57	0.57	7.88

1. PC1 = *PARAFAC* Component 1 fluorescence intensity score

2. Fractional difference = $DOM_{s\ in}\ CaCO_3$ (mg)/DOM_{aq} loss (mg).

DOM_s calculated as the sum of calcite removed by filtration and dissolution of residual crystals on vessel walls. Including Ca dissolution over-estimates DOM_s yield. DOM_s based on filtration slightly underestimates DOM yield (see supplementary spreadsheet).

Growth solution fluorescence measurements were conducted every 10 days in order to monitor $[DOM]_{aq}$ (as represented by PARAFAC component 1) throughout the experimental period (Fig. 54). $[DOM]_{aq}$ in the growth solution continuously declined in each beaker (Fig. 54a). After day 30, the rate of removal of DOM decreased in four of the treatments (low B, med A, med B and high A) and increased in two (low A and high B) (Fig. 45a).

Calcium ion concentrations in the growth solutions dropped throughout the experimental period for every treatment, indicating precipitation of calcium carbonate onto seeds (Fig. 54b). Fig. 45b shows consistent changes in the rates of calcium ion loss across treatments, except for the low [DOM] treatments, in which the removal rate of Ca^{2+}_{aq} was slower in the earlier parts of the experimental period. After day 30, Ca^{2+} removal from growth solution slowed in all solutions except Low A and High A. This reduction in growth rate corresponds

to the reduction in the rate of DOM_{aq} removal from day 30 to day 40 in most treatments, noted above. In most cases, changes in rate of DOM loss broadly resemble changes in rate of calcium ion loss; however, for the high B treatment DOM loss accelerates after day 30 while calcium ion loss decelerates.

Notably, more DOM_{aq} (by mass) was removed overall from the medium [DOM] treatments than the high [DOM] treatments. However, the organic carbon concentration was higher in crystals formed from the high [DOM] treatments (Fig. 6~~5~~a; Table 1). There was a notable colour transition from white crystals synthesised in deionised water growth solution (Fig. 6c) through to very dark-brown crystals in the high [DOM] precipitates, indicating that [DOM] in the parent solution has a significant impact on calcite colour. Log K_d values (Fig. 6~~5~~b) are similar for all treatments.

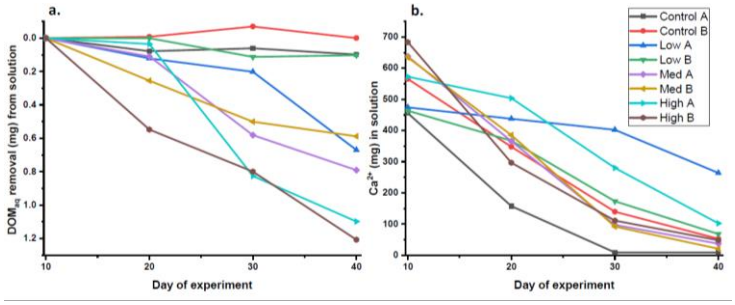

Fig. 5~~4~~. (a.) Fluorescence-inferred cumulative mass of DOM removal from the growth solutions, measured at 10-day intervals. Note reversed scale on the y-axis for ease of comparison with b. **b**.) FAAS-inferred Ca^{2+} measured at 10-day intervals within the growth-solution.

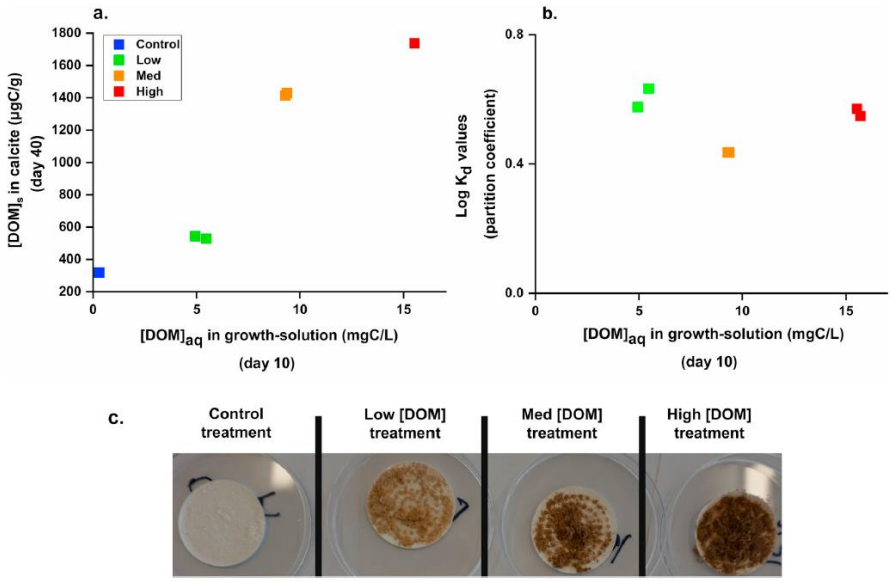

Fig. ~~5~~6. Results of duplicated calcite growth experiments using peatland DOM**. (a.)** $[DOM]_{aq}$ in the growth solution (day 10) is positively correlated with $[DOM]_s$ in the experimental calcite crystals. **(b.)** Log K_d (partition coefficient as a function of DOM incorporation) in the experimental calcite crystals (Log K_d values cannot be produced for the control treatment)**. (c.)** The crystals removed from the beakers upon completion of the experiment.~~.~~

Fig. ~~6~~7 shows final calcite yields for each [DOM] treatment. The calcite produced from the control treatment contained the lowest [DOM] of any of the samples. The final calcite yields for the low [DOM] treatments are variable, with low A producing a similar yield to the control treatments. Notably, the low A treatment also showed unusual behaviour in terms of the rate of reduction of calcium ions in solution (Fig. 5b). The ~~and~~ low B treatment ~~producing~~ produced a similar yield to the medium [DOM] treatments. Medium [DOM] treatments show significantly higher final calcite yields than control treatments. ~~The final calcite yields for the low [DOM] treatments are variable, with low A producing a similar~~

~~yield to the control treatments and low B producing a similar yield to the medium [DOM] treatments. Notably, the low A treatment also showed unusual behaviour in terms of the rate of reduction of calcium ions in solution (Fig. 4b).~~ The high [DOM] treatments are characterised by a reduction in final yield in comparison with the medium [DOM] treatments.

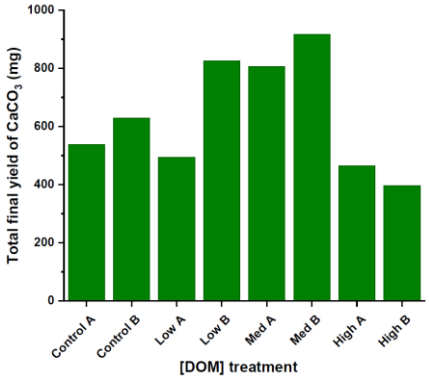

Fig. 7~~6~~. Total final calcite yield of each [DOM] treatment.

Fig. 8~~7~~ shows the 3D EEMs of the dissolved crystals. The fluorescence signal was dominated by humic-like peak C (ex 330-350 nm; em 420-480) (Coble, 1996), which increased as a function of higher DOM in the original growth solution. There was a notable lack of peak A (ex 250-260; em 380-480) compared to the fluorescence spectrum of the original growth solutions (Fig. A1; see section 4.5 for discussion).

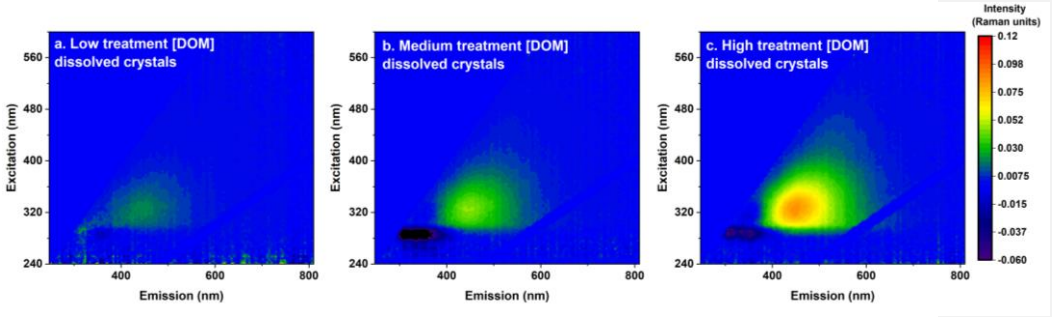

Fig. 8~~7~~. Composite 3D EEM spectra of dissolved crystals (mean EEM of crystals from replicates A and B).

3.3. Comparison to New Zealand dripwaters and flowstones

~~***Fig. 8.** (a.) Mean DOM concentrations (inferred by 3D EEM component 1 intensity score) in the cave dripwater*~~

Fig. 9. (a.) Mean DOM concentrations (inferred by 3D EEM component 1 intensity score) in the cave dripwater vs mean DOM values (inferred by 3D EEM component 1 intensity score) incorporated into the upper 3 mm of the flowstone calcite. Error bars represent standard deviation. **(b.)** Dripwater DOM vs log Kd values. Error bars represent standard deviation. Fig. 9. (c.) to (h.) shows the mean 3D EEM spectra from the dripwaters and flowstones from each site; **(c.)** Waipuna Cave dripwaters; **(d.)** Waipuna Cave flowstone; **(e.)** Hodges Creek Cave dripwaters **(f.)** Hodges Creek Cave flowstone; **(g.)** Dave's Cave dripwater; **(h.)** Dave's Cave flowstone.

The upper 3 mm of each natural cave flowstone was sampled at 1 mm resolution (Table A1), each sample (5 mg calcite to 4 mL solution) was dissolved using the same method as the experimentally produced calcite. The fluorescence analysis indicates a positive relationship between DOM in the dripwaters and the flowstones (Fig. 9~~8~~a), which complements the

results from our laboratory-based experiment. Fig. 98b shows the empirical partition coefficients for these samples (based on modern dripwater measurements). These partition coefficients are higher and more variable than those for the experimental treatments (Fig. 65b). ~~.~~ ~~–~~However, the absolute variability in K_d as a function of $[DOM]_{aq}$ across all measurements (speleothem and experimental) is small and does not display any correlation with $[DOM]_{aq}$.

The 3D EEM spectra shown in Fig. 9c to Fig. 9h. show variability between each cave site, as well as between flowstones and their parent dripwaters. Waipuna Cave's dripwaters contained relatively low [DOM] (Fig. 9a) with a weak fluorescence signal consistent with aromatic organic acids (humic-like), whilst the Waipuna Cave flowstone also contained a protein-like fluorescence signal, which is typically indicative of microbial activity. Hodges Creek Cave's flowstone and dripwaters contained much higher [DOM] than the other sites (Fig. 9a) and this is shown in the 3D EEM spectra (Fig. 9e, f). The dripwaters in Hodges Creek are predominantly humic-like (i.e. from the soil), yet the strongest fluorescence signal in the flowstones is protein-like, suggesting that microbial activity was an important contributor to the carbonate DOM signal. Dave's Cave flowstone and dripwaters have low [DOM] (Fig. 9a), the humic-like signal was visible in the dripwater (Fig. 9g), but weaker within the flowstone (Fig. 9h).

3.4. Calcite crystal morphology and DOM incorporation

Sample	High magnification (x 10,000)	Medium magnification (x 3-5,000)	Low magnification (x 300-500)
Reagent grade calcite	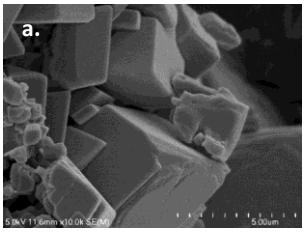	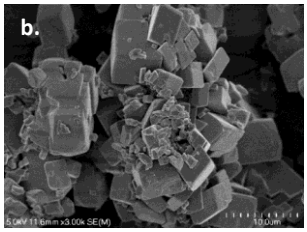	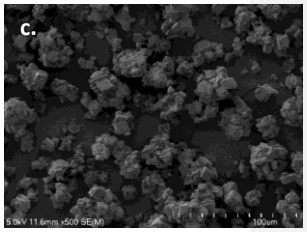

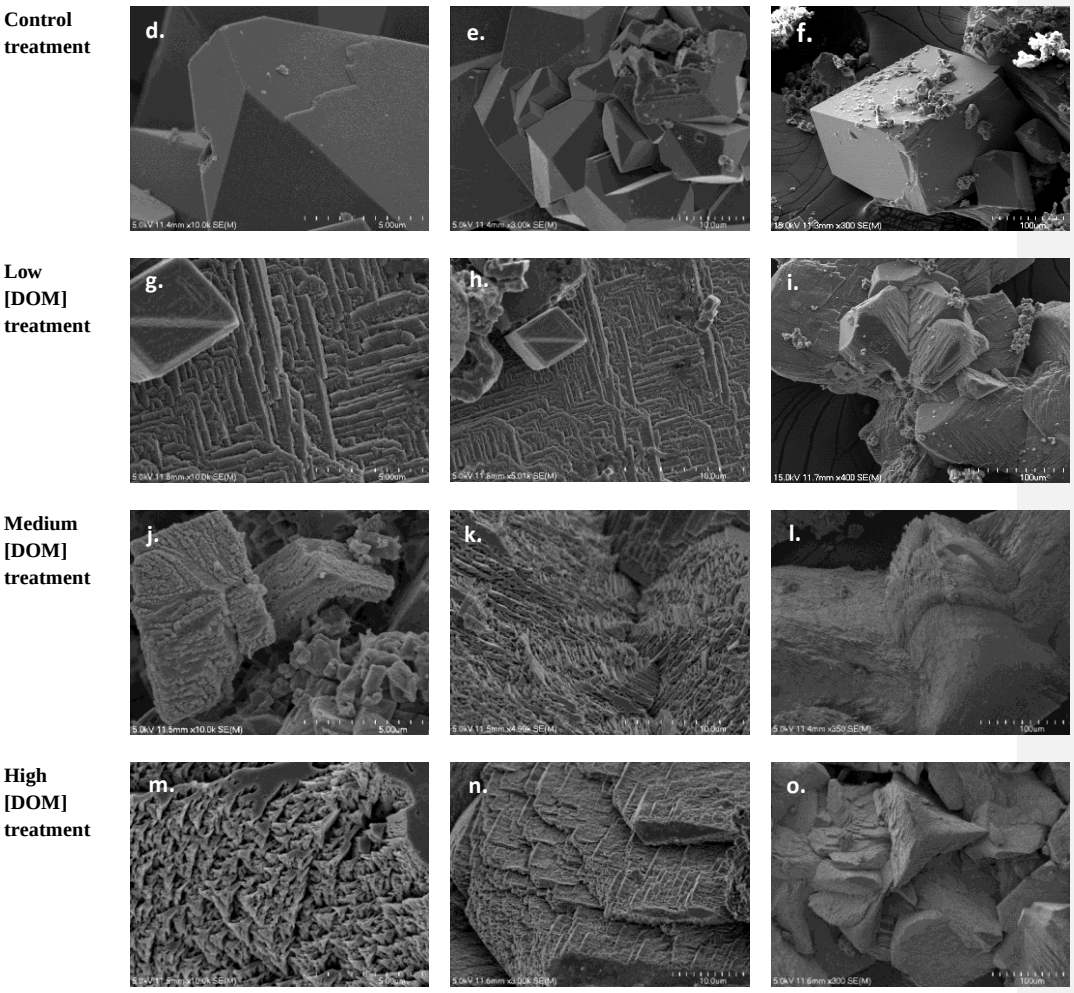

Fig. 10~~9~~. Representative SEM micrographs of seed crystals, control treatment crystals and crystals from low, medium and high [DOM] treatments.

3.4.1. Seed crystal morphology

The seed crystals (Fig. 10~~9~~a, b, c) show rhombohedral morphology, well-developed flat-faces and clearly defined edges and corners. There was some aggregation of the crystals, which were relatively uniform in size (<10 µm diameter; Fig. ~~9~~10a, b, c) and were notably smaller than the crystals that were synthesised during the experiment.

3.4.2. Control treatment crystal morphology

The control treatment yielded almost exclusively rhombohedral crystals (Fig. 10~~9~~d, e, f) which were symmetrical along the c-axis. The rhombohedra are characterised by well-defined flat faces with some macro-steps (Fig. 10~~9~~d, e). Aggregation of crystals occurred across a distribution of crystal sizes (Fig. ~~9~~10f). The most common size class had a width of 150-200 µm. The crystals produced in the control experiment solution were generally larger in size than those produced in the solutions containing DOM and strikingly similar to those obtained during abiotically mediated synthesis of calcium carbonate in the absence of exopolysaccharides and amino acids (Braissant et al., 2003).

3.4.3. Low [DOM] treatment crystal morphology

The crystals formed under low [DOM] conditions show generally rhombohedral morphology and rounded corners (Fig. 10~~9~~g, h). These crystals resemble the control [DOM] treatment crystals, apart from having rounded corners, which is symptomatic of the presence of organic matter (Frisia et al., 2018). Notably, there was a high density of sub-micron scale kinks on the crystal faces. The kinks could not have been produced during nucleation, as we seeded the experiments with rhombohedral calcite crystals prior to the experiment. They must therefore have been produced during the calcite growth process in the presence of DOM additives. In the calcite/DOM additive system, at low [DOM], there is clear evidence of habit modification and, based on purely morphological (SEM) observations, this seems to mostly affect the calcite (10-14) faces. This is similar to the effects of amino-acid additives (Orme et al., 2001). Furthermore, this experiment produced a clear range in crystal size. Fig. ~~9~~10i shows several aggregations of rhombohedral crystals with individual crystal diameters below 10 µm attached to much larger >50 µm prismatic crystals with morphological relief on their faces.

3.4.4. Medium [DOM] treatment crystal morphology

Fig. 10~~9~~k displays a point of aggregation between two crystals, which have very clear topographical relief. The crystals were of mixed sizes, and the larger crystals were prismatic, with less well-defined corners than crystals formed in the low [DOM] treatment.

3.4.5. High [DOM] treatment crystal morphology

Crystals formed from solution with high [DOM] were geometrically pyramidic and may have yielded both positive and negative rhombohedra. The crystals also have chiral morphologies due to step-effects. The crystals appear to have formed via aggregation with polymeric humic substances, incorporated as additives during nucleation and crystallisation. There was a diverse range of crystal orientations and sizes, but there was an upper size limit of 100 µm along the longest axis of individual crystals.

4. Discussion

4.1. Assessing the potential effects of [DOM] on $CaCO_3$ polymorph

Our experiment also allows us to assess the effect of [DOM] on the $CaCO_3$ polymorph. XRD and FTIRS analysis has determined that the synthesised crystals were calcite in each treatment. These data suggests that [DOM] up to ~15 mgC/L does not produce changes in $CaCO_3$ polymorphs during crystal growth, but rather drives calcite crystal morphogenesis (Cölfen and Antonietti, 2005). This finding may be consistent with a previous study, in which solutions containing 40 ~~ppm~~ mgC/L humic acids were shown to precipitate 25% vaterite (w/w) alongside calcite in synthetic seawater solutions (Falini et al., 2009).

4.2. The effect of [DOM] on crystal structure and growth

Based on the atomic absorption measurements of Ca^{2+}_{aq} at 10-day intervals through the experiment, the rate of crystallisation was relatively consistent across treatments (Fig. 5~~4~~b),

with crystallisation rates in most samples decreasing after day 30. It is reasonable to infer that this growth limitation was caused by the reduction of available calcium cations.

SEM images show a clear morphological variability between the crystals that were precipitated in low [DOM] growth solutions, and the crystals grown in high-concentration DOM growth solutions (Fig. 10~~9~~). In the low [DOM] treatment, aggregation of crystals is common. However, the fact that aggregation occurs across a range of crystal sizes indicates that aggregation is not associated with the presence of DOM but must have been promoted by physical or electrostatic interactions. Low [DOM] treatments show some kinks and steps in the morphology of the crystal faces, which, as noted above, must have formed during crystal growth from seeds. These may represent active growth sites where DOM may have been adsorbed. High [DOM] treatments showed a diverse range of orientations, perhaps due to sporadic nucleation events around DOM colloids in the crystal-growth solution, as opposed to more controlled nucleation surrounding the seed-crystals in the control and low [DOM] treatments (Fig. 10).

Defects can occur in crystal habits due to the presence of impurities (Frisia et al., 2000), which, in turn, can affect the thermodynamics and kinetics of growth (Frisia et al., 2000; Sangwal, 1996). An impurity is defined as a foreign substance other than the crystallizing compound (Sangwal, 1996). DOM is adsorbed to $CaCO_3$ via electrostatic bonding at the mineral-growth solution interface (Chalmin et al., 2012) through interacting anionic functional groups (COO^-, OH^-, and Ca^{2+}). SEM images imply that the presence of organic matter increases micron to sub-micron scale morphological step and kinks on individual crystal unit faces. Such irregularities were not present in the precipitates from the control treatments, within which rhombohedral flat-faced crystallites were synthesised, with both the positive and negative forms. Crystallites formed in the low [DOM] treatment were almost exclusively rhombohedral, with rounder corners than those produced in the control solution.

The medium and high [DOM] treatment produced crystals with positive and negative rhombohedra with chiral morphologies, and clear disruptions within the crystal lattice. These crystals were increasingly elongated compared to the low-concentration DOM crystal morphologies, with corners and pits and a high-step density.

4.3. DOM incorporation mechanisms and partition coefficients

There was a marked colour transition from white crystals synthesised in deionised water growth solution through to very dark-brown crystals in the high [DOM] precipitates (Fig. ~~A2~~5c, A2~~3~~). The implication that the change in colour was related to incorporation of DOM was supported by the fluorescence-derived measurements of the $[DOM]_s$ in the dissolved calcite. There was a positive, linear relationship between the [DOM] incorporated into the calcite and the [DOM] of the original growth solution (Fig. 6~~5~~). Furthermore, fluorescence measurements of the growth solution throughout the experiment showed that DOM was progressively removed through time (presumably via incorporation into/between the crystals).

Our results indicate that, during growth, the $CaCO_3$ crystals reliably incorporated a representative concentration of DOM from the parent solutions. These findings are consistent with those of Chalmin et al. (2012), in which a crystal growth experiment tested the incorporation of reagent grade humic acids into calcite. They aimed to use sulphur as a trace element for entrapped humic acids and found that humic acid incorporation into $CaCO_3$ was directly proportional to the amount of humic acid in the precipitating solution. This result is also consistent with the claim that dark colouring of speleothems is related to the incorporation of organic matter (Gázquez et al., 2012; Van Beynen et al., 2001).

Organic matter in speleothems can be accommodated either in extra-lattice positions at crystal boundaries or within defects of a single crystal. DOM may also be incorporated as

fluid inclusions (Ramseyer et al., 1997) and has been documented in 30-150 nm-wide pores in organically precipitated carbonate crystals between crystal subunits, as well as between individual crystals (Ramseyer et al., 1997). Ramseyer et al. (1997) suggested that, in the case of their study, DOM was incorporated during calcite growth but not within the lattice of carbonates. They were unable to firmly distinguish whether DOM was adsorbed onto the crystal surface or incorporated as aqueous fluid inclusions, though they suggested that a preferential adsorption onto crystal surfaces was the dominant mechanism (Ramseyer et al., 1997). An experimental study demonstrated that fulvic acids bind to calcite surfaces (Lee et al., 2005). Carboxyl groups ($COOH^-$) are common in natural DOM, and can readily be adsorbed onto calcite, which has a net positive charge (via Ca^{2+}). By contrast, an NMR (Nuclear Magnetic Resonance) spectroscopy study revealed that small organic (P containing) molecules can be incorporated in the calcite structure, thus supporting the notion that speleothems may provide a resilient record of organic matter present during crystallisation (Phillips et al., 2016). These results implied that calcite precipitated under natural conditions can accommodate organic molecules as structural defects.

SEM images of the crystals grown under increasing concentrations of DOM suggest a role for organic molecules in the morphogenesis of speleothem calcite. Increasing [DOM] results in increased density of observable steps and kinks at crystal surfaces, which may theoretically cause a positive feedback- loop of DOM incorporation in the form of fluid inclusions in the large number of pores visible in the crystals formed at high DOM concentrations (Fig. 10~~9~~m-o). Morphologies shown in Fig. 10~~9~~. for the medium and high DOM experiments are like those illustrated in Cölfen and Antonietti's (2005) seminal publication on mesocrystal (a superstructure of crystalline nanoparticles) formation, which sheds some light on the influence of DOM on the morphogenesis processes. In cave systems, nanocrystals and DOM form nanoparticles of approximately 3-4 nm (Fig. A5~~6~~), which can assemble to form a

mesoscale assemblage (i.e. a mesocrystal). Mesocrystals are characterised by voids between single nanoparticles, which may host organic matter. After completion of crystallographic fusion is reached (and a single crystal is formed) the organic matter can remain trapped at the boundaries between the former nanocrystals. High [DOM] may promote nano-inclusion in the amorphous phase, thus accommodating possible mismatches in nanocrystal lattices. Therefore, in the beakers containing [DOM] (but not in the blanks), there may have been a switch from a growth mechanism dominated by monomer-to-monomer attachment to a mechanism dominated by nano-particle attachment during the growth phase. Indeed, as there appears to be a linear relationship between DOM incorporation into the crystals and the quantity of the DOM in the original growth solution, we can confidently infer that DOM in cave waters influences the mechanisms of crystal growth, possibly including the formation of mesocrystals at the growth stage.

The determinant of morphological changes in our results appears to be [DOM]. Wynn et al. (2018) found that high crystal growth rates encouraged higher partition coefficients of sulphur into calcite due to increased defect sites on crystal surfaces (Wynn et al., 2018). This phenomenon was not clear in our experiment; however, positive Log K_d values (Fig. ~~5~~6b) showed that DOM_{aq} favours incorporation into calcite. The subtle preference for DOM inclusion in calcite seen through positive log K_d values may also be related to a selective bias towards incorporation of more aromatic hydrophobic DOM fractions into the calcite (Fig. ~~8~~7). A strong positive relationship between DOM hydrophilicity and peak A fluorescence intensity has previously been observed (Baker et al., 2008), and peak A fluorescence was notably absent in the precipitates. The fluorescence spectra of calcite dissolutions could be altered by acid dissolution of the calcite, because at low pH values (final pH of 5.6 in crystal digests) the protonation of acidic groups (including $–COO^-$) can cause reductions in fluorescence or result in other conformational changes (Hartland et al., 2010). However, such

artefacts did not account for the total absence of the peak A fluorophore (Fig. A6~~7~~), implying that the fluorescence moieties underlying this peak were not incorporated into/between the crystals.

Clearly, more work examining the partitioning of specific DOM molecules/fractions is required. However, while qualitative differences are apparent, calcite appears to faithfully record DOM solution concentrations. Further, these findings are important for interpreting trace metal signals in carbonates. Certain metal ions that are carried by aqueous DOM complexes are non-exchangeable on the timescale of typical thin-film residence times (Hartland et al., 2011). Therefore, DOM contained in speleothems may be tracked by the metals in these inert complexes where these can be shown to be irreversibly bound (Hartland et al., 2014).

4.4. [DOM] potential for growth inhibition at high concentrations

This study demonstrates that crystal growth may be inhibited when the crystallising fluids contain between 10 mgC/L ~~ppm~~ and 15 ~~ppm~~ mgC/L of [DOM], although the reliability of this interpretation is limited by only having two experimental replicates. Nevertheless, evidence for this occurrence has been demonstrated in other studies. An experimental calcite precipitation study (Inskeep and Bloom, 1986) demonstrated that 0.03- 0.14 mM L^{-1} (0.36 – 1.68 ~~ppm~~mg/L as C) of carbon water-soluble soil organic ligands (fulvic acids or soil extracts) can inhibit calcite growth. Complete inhibition of $CaCO_3$ precipitation has also been observed in an experimental study using growth solutions containing 80 mg/L~~ppm~~ of humic acids in synthetic sea water solutions (Falini et al., 2009), whilst the same study showed that 40 mg/L~~ppm~~ of humic acids reduced the amount of $CaCO_3$ precipitate by around 50% in synthetic sea water solutions (Falini et al., 2009) (although this phenomenon was also influenced by the presence of seawater ions). Hydrophobic acids from higher plants (filtered

at 0.1 µM) in the Florida Everglades have been shown to inhibit calcite growth rates by 50% in concentrations as low as 0.5 mg/L (Hoch et al., 2000). The same study demonstrated that DOM molecular weight and aromaticity correlated strongly with growth-inhibition, which was attributed to enhanced stereochemical effects on blocking active crystal growth sites.

In our study, the final yield of calcite crystals was significantly higher for the medium [DOM] treatment (805 mg (replicate A) and 916 mg (replicate B)) than for the control treatment (537 mg and 627 mg). However, the low [DOM] treatment showed significant variability, with replicate A producing 494 mg while replicate B produced 824 mg. The low A treatment also showed unusual behaviour compared to the other treatments in terms of the rates of loss of calcium ions from solution (Fig. 5~~4~~b). This may indicate an unforeseen problem with this treatment. However, given this variability in the low [DOM] treatment yields, at present we do not have enough data to clearly state the relationship between relatively low (<10 mgC/L~~ppm~~) concentrations of organic carbon in solution and calcite precipitation.

The high [DOM] treatment replicates produced 464 mg (replicate A) and 396 mg (replicate B) of calcite. This is significantly lower than the medium [DOM] treatments and similar to the control treatments. This may indicate that concentrations of organic carbon >10 ~~ppm~~ mgC/L tend to inhibit calcite precipitation. Additional replicates and treatments with even higher organic carbon concentrations would shed further light on this relationship.

4.5. Speleothems as archives of [DOM] and molecular characteristics

Speleothems exhibit different colours, and these changes have been predominantly attributed to organic matter content (Van Beynen et al., 2001; White, 1981). This was reinforced by our experiment, which showed a clear correlation between crystal colour and $[DOM]_s$ (Fig. ~~A2~~5c, A~~3~~2). Fluorescence analysis of dripwater and speleothems also indicated a strong positive

relationship between dripwater fluorescence and fluorescence of the upper 3 mm of speleothem sample, consistent with the findings in our experiment. This indicates that speleothems are a reliable recorder of [DOM] in cave waters, opening the possibility of using speleothems to reconstruct soil carbon leaching rates. However, there is a notable lack of a fluorescent ~~fulvic acid~~ peak A (hydrophilic DOM) in our 3D EEM spectrum of DOM_s from the dissolved experimental calcite (Fig. 8~~7~~). More research is required to understand the causes of this and how it may affect the interpretation of DOM measurements from speleothem calcite. There is also a lack of hydrophilic DOM fluorescence in the flowstones at each site (Fig. 9d, f, h). Hodge's Creek was the only site at which dripwater contained fluorescent hydrophilic and hydrophobic DOM (Fig. 9e), yet the DOM contained in the flowstone is dominated by protein-like (e.g. amino acid) fluorescence (Fig. 9f), indicating microbial/bacterial input of DOM or microbial/bacterial degradation of DOM. The Waipuna flowstone also shows a strong protein-like fluorescence signal (Fig. 9d). Dave's Cave dripwater (Fig. 9g) and flowstone (Fig. 9h) both had relatively weak fluorescence signals which were dominantly hydrophobic in nature. The differences in dripwater fluorescence properties between sites may be explained by vegetation and soil type overlying the caves, whilst microbial activity (leading to increased protein-like fluorescence) is likely to be heavily influenced by temperature, however further research is required to confirm these hypotheses.

The results of this experiment are consistent with previous studies (Chalmin et al., 2012; Falini et al., 2009), which have shown that organic matter captured by calcite precipitates in analogue experiments can be representative of the growth solution. However, our study expands on these results by assessing the effects of natural DOM, rather than those of laboratory-grade humic acids. The experiments have also revealed the effects that natural DOM concentrations have on calcite crystallite morphology.

Formatted: Font color: Auto

The most important piece of evidence for speleothem $[DOM]_s$ as a reliable proxy for cave water $[DOM]_{aq}$ is the positive, broadly linear relationship between $[DOM]_{aq}$ and $[DOM]_s$ in our experiment (Fig. 6~~5~~a). The partition coefficients are similar for all treatments, indicating that $[DOM]_s$ of calcite is a reliable proxy for the $[DOM]_{aq}$ of the original growth solution. However, there is a difference in the partition coefficients found for natural speleothems (Fig. 9~~8~~b) and our experimentally grown crystals (Fig. ~~5~~6b), with the natural speleothems being characterised by higher and more variable partition coefficients. Given the range of factors (e.g., calcite precipitation rate, DOM compositional changes, supersaturation, pH, microbial activity) potentially influencing this process within a cave environment, it is beyond the scope of the current study to ascertain the cause of this difference. Further, the K_d values calculated from the dripwater and flowstone samples (Fig. 9b) are likely to be relatively unreliable, given that the dripwater monitoring programme commenced potentially decades/hundreds of years after the precipitation of the flowstone sub-samples. However, the differences in log K_d values both between different speleothem samples and between the speleothems and the experimental treatments are small and do not display any correlation with [DOM]. Thus, it is reasonable to interpret speleothem DOM records as reflecting DOM concentrations in karst groundwater within the range of typical karst DOM concentrations (0-10 mgC/L~~ppm~~).

4.6 Crystal habits influenced by DOM_{aq}

Speleothem crystal habits have been used as proxies for drip-water supersaturation, presence of impurities and flow rates (Frisia et al., 2000), and to document diagenesis (Frisia et al., 2018). Indeed, calcite morphology in caves may be extremely complex, even when elements that are known to affect calcite morphology (such as Mg) are absent. Our study shows that crystal habits can be affected by [DOM] in the parent solution. Our results further suggest that the morphological relief (steps and kinks) in crystals formed at higher [DOM] may

enable the formation of fluid-inclusions (Fairchild and Baker, 2012), thus potentially increasing DOM incorporation (Ramseyer et al., 1997). Fluid inclusions of DOM may also have occurred in our experiments within the large pores and topographical relief visible in the crystals produced in the medium and high [DOM] growth solutions.

Our experiments provide evidence for growth inhibition of calcite crystals at DOM concentrations above 10 mgC/L~~ppm~~ (see above). The presence of impurities has long been known to inhibit calcite precipitation via adsorption of elemental impurities at crystal kinks (growth sites) (Meyer, 1984), whilst aqueous soil extracts and humic acid solutions have been found to inhibit calcite growth (Inskeep and Bloom, 1986).

The crystal morphologies in our controlled experiment were strongly influenced by [DOM]. Speleothem crystal habit has been related to a combination of supersaturation and flowrate (Gonzalez et al., 1992), the degree of saturation in our experiments was relatively consistent, so supersaturation is unlikely to have influenced differences in crystal habit between our samples. However, our experiment excluded many of the alternative factors (e.g. presence of Mg or Sr variation in supersaturation rate of the solution, drip rate variability) that are known to influence crystal habit in natural cave environments. Nevertheless, this is the first experimental work that unequivocally ties natural DOM concentration variability in cave-like waters to calcite crystal morphologies for conditions where the supersaturation state of the parent water may not vary considerably throughout the year and Mg concentration is negligible. The results of our experiments have wide implications for the interpretation of cave crystal morphologies in terms of parent water DOM concentrations.

4.7. Implications for carbonate sample selection

Formatted: Font: Bold

Our findings show further evidence that calcite fabric and colour can be strongly related to [DOM] incorporation. Researchers aiming to measure [DOM] in carbonates should undertake

visual and petrographic observations when selecting samples. Owing to the relationship between high [DOM] and topographical relief between crystals and crystal subunits., this approach to sample selection may be of value to fluid-inclusion-based research (e.g. clumped isotope analysis).

4.8~~7~~. Experiment limitations

Our experiment has several limitations that do not reflect natural cave environments. Notably, reagent grade calcite seed crystals that do not contain any DOM and are perfectly rhombohedral are extremely unlikely to occur in natural caves. The use of seed crystals may have somewhat altered the nature and characteristics of the encapsulating calcite crystals themselves. Our use of seed crystals also limits our ability to understand the nucleation processes of calcite crystals, and the effects that [DOM] may have on these processes. The experiment also excludes a range of natural occurrences in caves, such as microbial processes, changes in partial pressure, cave ventilation, temperature shifts and the presence of elements such as Mg and Sr. However, exclusion of these aforementioned factors was crucial in solely testing the effects of $[DOM]_{aq}$ on $[DOM]_s$ incorporation, calcite crystal morphology, and growth inhibition.

The K_d values that were calculated based on the flowstones and dripwaters are likely to be somewhat unreliable because the flowstone had precipitated prior (potentially decades to hundreds of years) to the collection of the feeding dripwaters. A future study could better measure K_d values in a natural environment by collecting dripwater [DOM] and sampling flowstones with faster growth rates than the flowstones used in this study.

Formatted: Subscript

Systematic controlled experiments could resolve many of the limitations of this study. For example; microbial organisms could be added to the growth-solutions, or growth-solutions with different DOM fractions (e.g. more protein-like, differing degrees of hydrophobicity), or

729 growth-solutions from different sources (e.g. from a forest soil or a tundra soil) could be
730 used. Growth-solutions could also be spiked with trace elements that are relevant to
731 speleothem palaeo-climate reconstructions (e.g. Sr, Mg), to test the relationship between
732 [DOM] and trace element incorporation into calcite.
733
734 Calcite crystals precipitated from solutions containing variable initial [DOM] showed
735 consistent variability in organic carbon content and crystal habit, as well as less consistent
736 variability in final crystal yield. We observed a positive, linear correlation between initial
737 organic carbon concentration in solution and final organic carbon concentration in calcite,
738 with log K_d values of around 0.5. Crystals produced in 0 mgC/L~~ppm~~ DOM solutions were
739 rhombohedral, white in colour and had very low fluorescence when dissolved in dilute HCl.
740 In the low DOM treatment, small (<10 µm) rhombohedral crystallites with rounded corners
741 were produced in aggregates, yet there were also much larger, prismatic crystals. Crystals that
742 were synthesised in the medium and high DOM treatments were also prismatic with many
743 steps and kinks. This may have important implications for interpreting the causes behind
744 variability in crystal habit and fabric in speleothems, which have been previously utilised as
745 proxies of hydrology and hydro-climatology.

746 Further calcite crystal growth experiments from parent solutions containing organic matter
747 with different molecular characteristics should be undertaken to test preferential adsorption of
748 different molecular constituents of DOM and the potential associated effects on crystal habit.
749 For example, our study shows an absence of fluorescence peak A in the dissolved calcite.
750 More research focusing on isolated DOM fractions should be undertaken to determine the
751 reliability of calcite incorporation.

752 **6. Funding**

This study was made possible by Royal Society of New Zealand Te Apārangi, Marsden Fund Grant UOW1403 and Rutherford Discovery Fellowship award RDF-UOW1601 (AH) and the Australian Research Council (grant DP160101058) (SF).

7. Acknowledgements

We would like to acknowledge Joshua L. Ratcliffe and Associate Professor David Campbell (University of Waikato) for assistance in collecting the peat water from Kopuatai bog, Dr John C. Hellstrom (University of Melbourne) and Travis Cross (University of Auckland) for assistance in flowstone sample collection. Thanks to the Department of Conservation for allowing us to access and sample from Dave's Cave and Hodges Creek Cave (Research and Collection Permit 37934-GEO), and Pete and Libby Chandler for allowing us to access and sample from dripwaters and flowstones within Waipuna Cave and supporting our ongoing monitoring campaigns. Thanks to Helen Turner for assistance in using the SEM, Kirsty Vincent for help using the XRD and Steven Newcombe (all based at the University of Waikato) for producing the alterations to the glassware used in the experiment.

References:

Affolter, S., et al., 2019. Central Europe temperature constrained by speleothem fluid inclusion water isotopes over the past 14,000 years. Sci. Adv. 5 (6), eaav3809.

Andersson, C.A., Bro, R., 2000. The N-way toolbox for MATLAB. Chemometrics and Intelligent Laboratory Systems 52 (1), 1–4.

Baker, A., Barnes, W., Smart, P.L., 1996. Speleothem luminescence intensity and spectral characteristics: signal calibration and a record of palaeovegetation change. Chem. Geol. 130 (1–2), 65–76.

Baker, A., et al., 1999. Stalagmite luminescence and peat humification records of palaeomoisture for the last 2500 years. Earth Planet. Sci. Lett. 165 (1), 157–162.

Baker, A., Tipping, E., Thacker, S.A., Gondar, D., 2008. Relating dissolved organic matter fluorescence and functional properties. Chemosphere 73 (11), 1765–1772.

Blyth, A.J., Asrat, A., Baker, A., Gulliver, P., Leng, M.J., Genty, D., 2007. A new approach to detecting vegetation and land-use change using high-resolution lipid biomarker records in stalagmites. Quatern. Res. 68 (3), 314–324.

Blyth, A.J., Hartland, A., Baker, A., 2016. Organic proxies in speleothems – New developments, advantages and limitations. Quat. Sci. Rev. 149, 1–17.

Borsato, A., Frisia, S., Fairchild, I.J., Somogyi, A., Susini, J., 2007. Trace element distribution in annual stalagmite laminae mapped by micrometer-resolution X-ray fluorescence: implications for incorporation of environmentally significant species. Geochim. Cosmochim. Acta 71 (6), 1494–1512.

Braissant, O., Cailleau, G., Dupraz, C., Verrecchia, E.P., 2003. Bacterially induced mineralization of calcium carbonate in terrestrial environments: the role of exopolysaccharides and amino acids. J. Sediment. Res. 73 (3), 485–490.
Caldwell, J., Davey, A.G., Jennings, G.N., Spate, A.P., 1982. Colour in some Nullarbor Plain speleothems. Helictite 20 (1), 3–10.
Chalmin, E., Perrette, Y., Fanget, B., Susini, J., 2012. Investigation of organic matter entrapped in synthetic carbonates - a multimethod approach. Microsc. Microanal. 19, 132–144.
Charman, D.J., et al., 2001. Paleohydrological records from peat profiles and speleothems in Sutherland, northwest Scotland. Quat. Res. 55 (2), 223–234.
Coble, P.G., 1996. Characterization of marine and terrestrial DOM in seawater using excitation-emission matrix spectroscopy. Mar. Chem. 51 (4), 325–346.
Coble, P.G., Del Castillo, C.E., Avril, B., 1998. Distribution and optical properties of CDOM in the Arabian Sea during the 1995 Southwest Monsoon. Deep-Sea Res. II Top. Stud. Oceanogr. 45 (10), 2195–2223.
Cole, J.J., Caraco, N.F., Kling, G.W., Kratz, T.K., 1994. Carbon dioxide supersaturation in the surface waters of lakes. Science 265 (5178), 1568–1570.
Cole, J.J., et al., 2007. Plumbing the global carbon cycle: integrating inland waters into the terrestrial carbon budget. Ecosystems 10 (1), 172–185.
Colfen, H., Antonietti, M., 2005. Mesocrystals: inorganic superstructures made by highly parallel crystallization and controlled alignment. Angew. Chem. Int. Ed. 44 (35), 5576–5591.
Evans, C.D., Monteith, D.T., Cooper, D.M., 2005. Long-term increases in surface water dissolved organic carbon: observations, possible causes and environmental impacts. Environ. Pollut. 137 (1), 55–71.
Evans, C.D., Chapman, P.J., Clark, J.M., Monteith, D.T., Cresser, M.S., 2006. Alternative explanations for rising dissolved organic carbon export from organic soils. Glob. Chang. Biol. 12 (11), 2044–2053.
Fairchild, I.J., Baker, A., 2012. Speleothem Science: From Process to Past Environments. John Wiley, Chichester, U.K.
Falini, G., Fermani, S., Tosi, G., Dinelli, E., 2009. Calcium carbonate morphology and structure in the presence of seawater ions and humic acids. Crystal Growth and Design 9 (5), 2065–2072.
Fellman, J.B., Hood, E., Spencer, R.G.M., 2010. Fluorescence spectroscopy opens new windows into dissolved organic matter dynamics in freshwater ecosystems: a review. Limnol. Oceanogr. 55 (6), 2452–2462.
Freeman, C., Evans, C.D., Monteith, D.T., Reynolds, B., Fenner, N., 2001. Export of organic carbon from peat soils. Nature 412, 785.
Freeman, C., et al., 2004. Export of dissolved organic carbon from peatlands under elevated carbon dioxide levels. Nature 430 (6996), 195.
Frisia, S., Borsato, A., Fairchild, I.J., McDermott, F., 2000. Calcite fabrics, growth mechanisms, and environments of formation in speleothems from the Italian Alps and southwestern Ireland. J. Sediment. Res. 70 (5), 1183–1196.
Frisia, S., Borsato, A., Hellstrom, J., 2018. High spatial resolution investigation of nucleation, growth and early diagenesis in speleothems as exemplar for sedimentary carbonates. Earth Sci. Rev. 178, 68–91.
Gazquez, F., Calaforra, J.M., Rull, F., Forti, P., Garcia-Casco, A., 2012. Organic matter of fossil origin in the amberine speleothems from El Soplao Cave (Cantabria, Northern Spain). Int. J. Speleol. 41 (1), 113–123.
Genty, D., et al., 2001. Dead carbon in stalagmites: Carbonate bedrock paleodissolution vs. ageing of soil organic matter. Implications for 13C variations in speleothems. Geochim. Cosmochim. Acta 65 (20), 3443–3457.
Gilmore, A.M., Cohen, S.M., 2013. Analysis of the chromophoric dissolved organic matter in water by EEMs with Horiba-Jobin Yvon fluorescence instrument called. Aqualog. Readout 41, 19–24.
Gonzalez, L.A., Carpenter, S.J., Lohmann, K.C., 1992. Inorganic calcite morphology: roles of fluid chemistry and fluid flow. J. Sediment. Res. 62 (3), 382–399.
Gruzensky, P., 1967. Growth of calcite crystals. Cryst. Growth 365–367.
Hartland, A., Zitoun, R., 2018. Transition metal availability to speleothems controlled by organic binding ligands. Geochemical Perspectives: Letters 8, 22–25.

847 Hartland, A., Fairchild, I.J., Lead, J.R., Baker, A., 2010. Fluorescent properties of organic
848 carbon in cave dripwaters: effects of filtration, temperature and pH. Sci. Total
849 Environ. 408 (23), 5940–5950.
850 Hartland, A., Fairchild, I.J., Lead, J.R., Zhang, H., Baalousha, M., 2011. Size, speciation
851 and lability of NOM–metal complexes in hyperalkaline cave dripwater. Geochim.
852 Cosmochim. Acta 75 (23), 7533–7551.
853 Hartland, A., Fairchild, I.J., Lead, J.R., Baker, A., Frisia, S., Baalousha, M. 2012. From soil to cave:
854 transport of trace metals by natural organic
855 matter in karst dripwaters. Chem. Geol. 304, 68–82.
856 Hartland, A., Fairchild, I.J., Muller, W., Dominguez-Villar, D., 2014. Preservation of
857 NOM-metal complexes in a modern hyperalkaline stalagmite: implications for speleothem
858 trace element geochemistry. Geochim. Cosmochim. Acta 128, 29–43.
859 Hill, C.A., Forti, P., Shaw, T.R., 1997. Cave Minerals of the World. National Speleological
860 Society, Huntsville, AL.
861 Hoch, A.R., Reddy, M.M., Aiken, G.R., 2000. Calcite crystal growth inhibition by humic
862 substances with emphasis on hydrophobic acids from the Florida Everglades.
863 Geochim. Cosmochim. Acta 64 (1), 61–72.
864 Inskeep, W.P., Bloom, P.R., 1986. Kinetics of calcite precipitation in the presence of water
865 soluble organic ligands. Soil Sci. Soc. Am. J. 50, 1167–1172.
866 Ishii, S.K.L., Boyer, T.H., 2012. Behavior of reoccurring PARAFAC components in fluorescent
867 dissolved organic matter in natural and engineered systems: a critical review.
868 Environ. Sci. Technol. 46 (4), 2006–2017.
869 Lead, J.R., Wilkinson, K.J., 2006. Aquatic colloids and nanoparticles: current knowledge
870 and future trends. Environ. Chem. 3 (3), 159–171.
871 Lechleitner, F.A., Dittmar, T., Baldini, J.U.L., Prufer, K.M., Eglinton, T.I., 2017. Molecular
872 signatures of dissolved organic matter in a tropical karst system. Org. Geochem. 113,
873 141–149.
874 Lee, Y.J., Elzinga, E.J., Reeder, R.J., 2005. Cu (II) adsorption at the calcite–water interface
875 in the presence of natural organic matter: kinetic studies and molecular-scale
876 characterization. Geochim. Cosmochim. Acta 69 (1), 49–61.
877 Leenheer, J.A., Croue, J.-P., 2003. Characterizing aquatic dissolved organic matter.
878 Environ. Sci. Technol. 37, 18A–26A.
879 Lehmann, J., Kleber, M., 2015. The contentious nature of soil organic matter. Nature 528
880 (7580), 60–68.
881 Mavromatis, V., et al., 2017. Effect of organic ligands on Mg partitioning and Mg isotope
882 fractionation during low-temperature precipitation of calcite in the absence of
883 growth rate effects. Geochim. Cosmochim. Acta 207, 139–153.
884 Mayorga, E., et al., 2005. Young organic matter as a source of carbon dioxide outgassing
885 from Amazonian rivers. Nature 436, 538.
886 Meyer, H.J., 1984. The influence of impurities on the growth rate of calcite. J. Cryst.
887 Growth 66 (3), 639–646.
888 Monteith, D.T., et al., 2007. Dissolved organic carbon trends resulting from changes in
889 atmospheric deposition chemistry. Nature 450 (7169), 537–540.
890 Monteith, D.T., Evans, C.D., Henrys, P.A., Simpson, G.L., Malcolm, I.A., 2014. Trends in
891 the hydrochemistry of acid-sensitive surface waters in the UK 1988–2008. Ecol. Indic.
892 37, 287–303.
893 Murphy, K.R., Stedmon, C.A., Graeber, D., Bro, R., 2013. Fluorescence spectroscopy and
894 multi-way techniques. PARAFAC. Anal. Methods 5 (23), 6557–6566.
895 Nagra, G., et al., 2017. Dating stalagmites in Mediterranean climates using annual trace
896 element cycles. Sci. Rep. 7 (1), 621.
897 Ni, M., Ratner, B.D., 2008. Differentiating calcium carbonate polymorphs by surface
898 analysis techniques—an XPS and TOF-SIMS study. Surf. Interface Anal. 40 (10),
899 1356–1361.
900 Nielsen, M.H., Aloni, S., De Yoreo, J.J., 2014. In situ TEM imaging of CaCO3 nucleation
901 reveals coexistence of direct and indirect pathways. Science 345 (6201), 1158–1162.
902 Orme, C.A., et al., 2001. Formation of chiral morphologies through selective binding of
903 amino acids to calcite surface steps. Nature 411 (6839), 775.
904 Perrette, Y., et al., 2015. Determining soil sources by organic matter EPR fingerprints in
905 two modern speleothems. Org. Geochem. 88, 59–68.
906 Phillips, B.L., Zhang, Z., Kubista, L., Frisia, S., Borsato, A., 2016. NMR spectroscopic study

of organic phosphate esters coprecipitated with calcite. Geochim. Cosmochim. Acta 183, 46–62.
Quiers, M., Perrette, Y., Chalmin, E., Fanget, B., Poulenard, J., 2015. Geochemical mapping of organic carbon in stalagmites using liquid-phase and solid-phase fluorescence. Chem. Geol. 411, 240–247.
Rae, R., Howard-Williams, C., Hawes, I., Schwarz, A.-M., Vincent, W.F., 2001. Penetration of solar ultraviolet radiation into New Zealand lakes: influence of dissolved organic carbon and catchment vegetation. Limnology 2 (2), 79–89.
Ramseyer, K., et al., 1997. Nature and origin of organic matter in carbonates from speleothems, marine cements and coral skeletons. Org. Geochem. 26 (5–6), 361–378.
Ratcliffe, J.L., Campbell, D.I., Clarkson, B.R., Wall, A.M., Schipper, L.A., 2019. Water table fluctuations control CO2 exchange in wet and dry bogs through different mechanisms. Sci. Total Environ. 655, 1037–1046.
Rutlidge, H., et al., 2014. Dripwater organic matter and trace element geochemistry in a semi-arid karst environment: implications for speleothem paleoclimatology. Geochim. Cosmochim. Acta 135, 217–230.
Sangwal, K., 1996. Effects of impurities on crystal growth processes. Prog. Cryst. Growth Charact. Mater. 32 (1), 3–43.
Sauve, S., Hendershot, W., Allen, H.E., 2000. Solid-solution partitioning of metals in contaminated soils: dependence on pH, total metal burden, and organic matter. Environ. Sci. Technol. 34 (7), 1125–1131.
Schmidt, M.W.I., et al., 2011. Persistence of soil organic matter as an ecosystem property. Nature 478, 49.
Scroxton, N., et al., 2018. Rapid measurement of strontium in speleothems using corescanning micro X-ray fluorescence. Chem. Geol. 487, 12–22.
Stanley, E.H., Powers, S.M., Lottig, N.R., Buffam, I., Crawford, J.T., 2012. Contemporary changes in dissolved organic carbon (DOC) in human-dominated rivers: is there a role for DOC management? Freshw. Biol. 57, 26–42.
Stedmon, C.A., Bro, R., 2008. Characterizing dissolved organic matter fluorescence with parallel factor analysis: a tutorial. Limnol. Oceanogr. Methods 6 (11), 572–579.
Sulatskaya, A.I., Maskevich, A.A., Kuznetsova, I.M., Uversky, V.N., Turoverov, K.K., 2010. Fluorescence quantum yield of thioflavin T in rigid isotropic solution and incorporated into the amyloid fibrils. PLoS One 5 (10), e15385.
Van Beynen, P., Bourbonniere, R., Ford, D., Schwarcz, H., 2001. Causes of colour and fluorescence in speleothems. Chem. Geol. 175 (3–4), 319–341.
White, W.B., 1981. Reflectance spectra and colour in speleothems. National Speleological Society Bulletin 43 (1), 20–26.
Williams, P.W., Marshall, A., Ford, D.C., Jenkinson, A.V., 1999. Palaeoclimatic interpretation of stable isotope data from Holocene speleothems of the Waitomo district, North Island, New Zealand. The Holocene 9 (6), 649–657.
Wynn, P.M., et al., 2018. Sulphate partitioning into calcite: Experimental verification of pH control and application to seasonality in speleothems. Geochim. Cosmochim. Acta 226, 69–83.

957

958

959

960

961

962

963

964

965

966

967

968

969

970

971

972

973

974

975

976

APPENDIX

Formation of calcite in the presence of dissolved organic matter: partitioning, fabrics and fluorescence

Andrew R. Pearson[1*], Adam Hartland[1], Silvia Frisia[2], Bethany R.S. Fox[3,1].

[1] Environmental Research Institute, School of Science, Faculty of Science and Engineering, University of Waikato, Hamilton, 3216, New Zealand.

[2] School of Environmental and Life Sciences, The University of Newcastle, Callaghan, New South Wales, 2308, Australia.

[3] Department of Biological and Geographical Sciences, University of Huddersfield, Huddersfield, HD1 3DH, United Kingdom.

*Corresponding author: apearson181@gmail.com

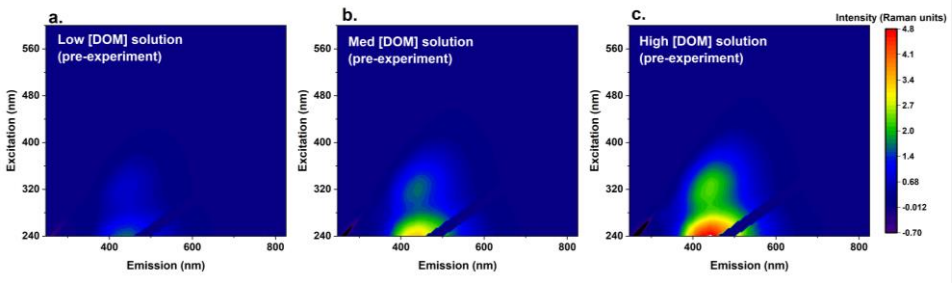

Fig. A1. 3D excitation-emission matrices of diluted peat-water solutions prior to crystal growth experiment.

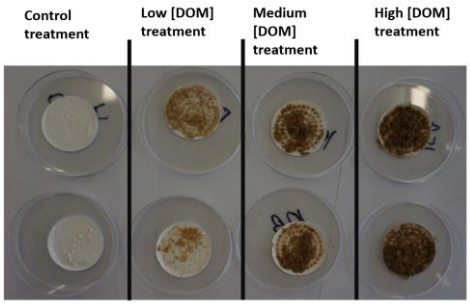

Fig. A2~~3~~. Birds-eye view of beaker 'A' of Control, Low, Medium, High DOM treatments shortly after completion of the experiment on day 40.

Table A1. Cave dripwater samples and dissolved speleothem subsamples used in the composite 3D EEMs.

Field-site locations of flowstones	N of dripwater samples	N of dissolved $CaCO_3$ fluorescence-inferred DOM measurements
Dave's Cave (Fiordland, South Island, New Zealand).	2	3 (upper 3 mm)
Hodges Creek (Kahurangi National Park, South Island, New Zealand).	5	3 (1,3,4 mm (no 2 mm subsample available)
Waipuna (Waitomo region, North Island, New Zealand).	32	3 (upper 3 mm)

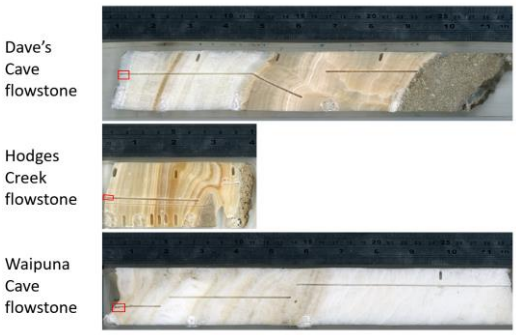

996

997 **Fig. A3~~4~~.** Three flowstones from New Zealand displaying different colours that may be reflective of DOM
998 incorporation. The red square marks the upper 3 mm from which fluorescence comparisons were made against
999 dripwaters.

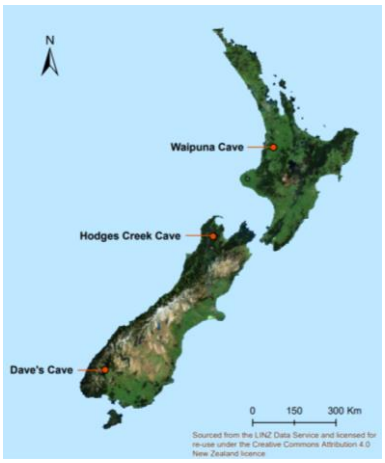

1000

1001 **Fig. A~~5~~4**. Location of the cave sites within New Zealand.

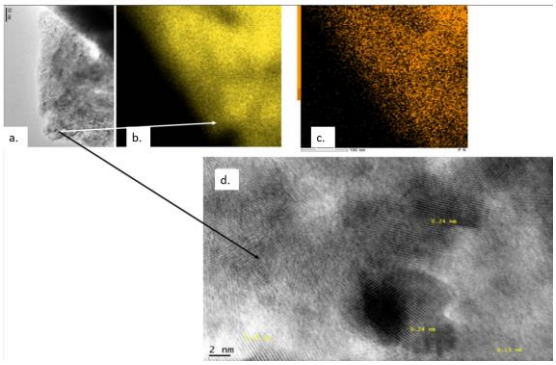

Fig. A~~6~~5. TEM images of a precipitate from Rumbling Gut cave, Waitomo, N. Island, New Zealand. (a.) is the whole particle; (b.) a Ca map of the particle; (c.) a P map of the particle; and (d.) nanocrystal aggregation. The particle formed on a TEM grid where a drop of cave dripwater was left overnight to degas in a plastic vial. The particle was produced under a low drip-rate, which is common under low recharge conditions. The medium onto which the calcite (as determined by d-spacing of 2.4 Angstrom (d), the Ca composition (insert b)) precipitated is a C film on a copper grid. The result is an array of nanocrystals with lattices mismatched, bridged by amorphous material, which appears to consist of C and P, as well as Si. A reasonable interpretation is that colloidal particulate (Si, Al, C, P) was adsorbed onto the C grid and then the nanocrystal nucleation was favoured by the presence of colloids. These bridged the nanocrystals, which have a random orientation, most likely given by the amorphous C substrate. In the case of speleothems, where the substrate is already CaCO3 crystals, or our experiments (calcite seeds), it is more likely that the aggregates of nanocrystal found a suitable, active crystalline substrate that favoured their orientation. The colloidal particulate remained trapped between the nanocrystals.

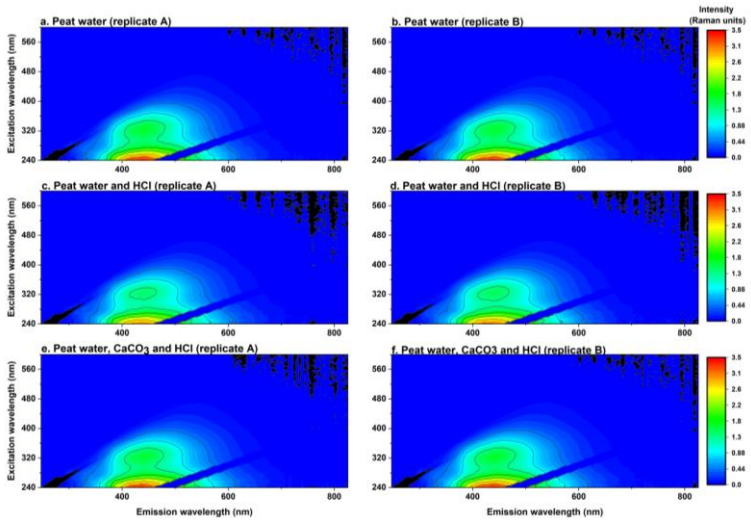

Fig. A~~7~~6. 3D EEM spectra of Peat water (a., b.); Peat water and HCl (c., d.); and Peat water, dissolved $CaCO_3$ and HCl (e., f.).